

# Elliptic flow from a parton cascade

Bin Zhang<sup>a</sup>, Miklos Gyulassy<sup>b</sup>, and Che Ming Ko<sup>a</sup>

<sup>a</sup> *Cyclotron Institute and Physics Department,*

*Texas A&M University, College Station, TX 77843-3366, USA*

<sup>b</sup> *Physics Department, Columbia University,*

*New York, NY 10027, USA*

(February 5, 1999)

## Abstract

The dependence of elliptic flow at RHIC energies on the effective parton scattering cross section is calculated using the ZPC parton cascade model. We show that the  $v_2$  measure of elliptic flow saturates early in the evolution before the hadronization transition to a rather large value  $\sim 0.05 - 0.15$  as  $\sigma_g$  varies from 2-10 mb and thus is a sensitive probe of the dynamics in the plasma phase.

25.75.Ld, 24.10.Jv, 24.10.Lx

In nucleus-nucleus collisions at the Relativistic Heavy Ion collider (RHIC), a system of deconfined quarks and gluons is expected to be produced for about  $3 - 10$  fm/c [1]. Various signatures have been proposed to verify its existence [2]. Since the volume and lifetime of this matter may be much larger and longer than those given by the confinement scale  $\approx 1/\Lambda_{QCD}$ , it is expected that collective motion of these deconfined partons should arise and have observable consequences that provide information on the dynamics in quark gluon plasma.

The collective motion of particles in heavy ion collisions can be studied via directed and elliptic flows. The directed flow, which measures the collective motion of particles in the reaction plane, has been studied extensively at BEVALAC, SIS, and AGS energies and found to be appreciable [3–6]. It becomes small at higher energies due to the large beam rapidity. In this case, it is more suitable to study the elliptic flow [7,8], which measures the azimuthal asymmetry of the transverse flow pattern. For heavy ion collisions with fixed targets, such as at CERN SPS, elliptic flow is generated by hadronic final state interactions [8]. On the other hand, at RHIC energies and beyond, copious mini-jet production leads to a high density of partons on a very short time scale and elliptic flow can be generated from interactions at the partonic level prior to hadronization. The aim of this letter is to calculate this effect using the parton cascade code ZPC [9,10].

Initial partonic conditions can be estimated for Au-Au collisions at RHIC energies via the HIJING generator [11] for example. Here we will consider simple idealized geometries for a first analysis. Initially, partons are uniformly distributed in the overlapping region of two disks each having a transverse radius of 5 fm with their centers separated by a distance equal to the impact parameter. For collisions of large nuclei at not very large impact parameters, the multiplicity is roughly proportional to the overlapping area. HIJING estimates for  $b = 0$  a gluon rapidity density  $dN_g/dy \approx 300$ . Again as a first idealization we assume a uniform rapidity distribution from  $-5$  to  $+5$  and take a momentum distribution given by a local thermal one at a temperature of 500 MeV. Furthermore, produced particles are taken to be formed on a hyperbola in the  $t$ - $z$  plane, with  $z$  the beam direction and  $x$ - $z$  plane the reaction

plane, using a formation proper time  $\tau_0 = 0.2$  fm.

At RHIC energies, the initial minijet system is dominated by gluons. Their subsequent time evolution can be described by the parton cascade model ZPC. In this model, only gluon-gluon elastic scattering has been included, with a cross section

$$\frac{d\sigma_g}{dt} = \frac{9\pi\alpha^2}{2} \left(1 + \frac{\mu^2}{s}\right) \frac{1}{(t - \mu^2)^2}.$$

In the above, the strong interaction coupling constant  $\alpha$  is taken to be 0.47, and  $\mu$  is an effective screening mass responsible for regulating the divergent leading-order cross section. We vary  $\mu$  to study the dependence of the elliptic flow on  $\sigma_g$ .

The elliptic flow of partons is characterized by the second Fourier coefficient  $v_2$  in their momentum distribution, i.e.,

$$\frac{1}{N} \frac{dN}{d\phi} = v_0 + 2v_1 \cos(\phi) + 2v_2 \cos(2\phi) + \dots \quad (1)$$

Alternatively, it can be characterized by  $v'_2$  in the expansion of their transverse energy distribution,

$$\frac{1}{\langle E_T \rangle} \frac{dE_T}{d\phi} = v'_0 + 2v'_1 \cos(\phi) + 2v'_2 \cos(2\phi) + \dots \quad (2)$$

Numerically,  $v_2$  is measured by averaging

$$\cos(2\phi) = \frac{p_x^2 - p_y^2}{p_x^2 + p_y^2}$$

over partons, i.e., it is the single particle average of squared transverse momentum asymmetry. Similarly,  $v'_2$  is measured by the  $E_T$  weighted single particle average of  $\cos(2\phi)$ . In general, the two azimuthal distributions do not have to be the same, and the two coefficients  $v_2$  and  $v'_2$  are thus not necessarily equal [12]. We will later give an example in which they develop different values.

The elliptic flow arises due to multiple collisions as long as the initial transverse spatial distribution is azimuthally asymmetric. For fixed impact parameters, its value reflects the strength of interactions ( $\sigma_g$ ). For fixed  $\sigma_g$  its value depends on the spatial asymmetry as a function of the impact parameter (or multiplicity).

In Fig. 1, we first show results for fixed impact parameter  $b = 7.5$  fm. The time evolution of  $v_2$  for different values of the gluon-gluon scattering cross section is shown. Note that all asymptotic values are reached very early,  $t < 2$  fm/c, well before the hadronization transition. For interaction length  $\sqrt{\sigma/\pi}$  larger than the mean free path, the numerical method of particle partition [13] has been used in order to obtain stable solutions of the Boltzmann equation. For the typical cross section between gluons, 3 mb, the final  $v_2$  after the partonic stage is around 0.1 which is quite “large” and easily detectable. Since the screening mass, or equivalently, the effective parton scattering cross section is uncertain we study its effect on the elliptical flow by using different values for the cross section, i.e., 1 mb and 10 mb. We see that  $v_2$  is rather sensitive to the cross section. This demonstrates that very large dissipative corrections are at work since in the ideal fluid limit the flow depends only on the speed of sound that is in our case  $1/\sqrt{3}$ . The important role played by dissipative phenomena in collective properties of plasma evolution was also demonstrated in [10] in connection with the transverse energy evolution. For these initial conditions even Navier-Stokes is inadequate and the full microscopic parton cascade is necessary. The strong dependence of the elliptic flow on the parton cross section could provide an important probe of the plasma dynamics if hadronization and final hadronic rescatterings do not modify the results too much. We cannot yet address this problem within the scope of ZPC and leave that important topic to a future study.

In Fig. 2, we compare the time evolution of  $v_2$  and  $v'_2$  for a gluon-gluon cross section of 10 mb. The statistical errors are denoted by bars. We see that  $v'_2$  is always distinctively larger than  $v_2$  during the evolution. It indicates that particles moving in the  $x$  direction tend to have relatively larger  $E_T$  than particles moving in the  $y$  direction. Even though final-state particle production may change the difference, this gives an example of different values for  $v_2$  and  $v'_2$ . The difference between  $v_2$  and  $v'_2$  becomes less significant when the cross section becomes smaller.

To study how the elliptic flow reflects the collision geometry, we show in Fig. 3 the dependence of the elliptic flow on the impact parameter for medium range impact parameters. An

almost linear dependence is observed, and this is similar to the impact parameter dependence obtained from the hydrodynamic model [8]. The linear increase of elliptic flow as a function of impact parameter reflects the initial spatial asymmetry, which can be characterized, e.g., by the width  $L_x$  and height  $L_y$  of the overlapping region, via  $\alpha_s = (L_y - L_x)/(L_y + L_x)$ . One can easily show that for medium range impact parameters, the spatial asymmetry is approximately linearly proportional to the impact parameter, similar to the impact parameter dependence of the elliptical flow. However, for  $b/(2R)$  very close to 1, the spatial asymmetry approaches 1, but the  $v_2$  coefficient actually drops to 0. This is simply due to the fact that there are too few particles which can undergo scattering to develop a momentum asymmetry from the spatial asymmetry. In Fig. 4, the time evolution of  $v_2$  is shown for different impact parameters. Although collisions at larger impact parameter give rise to a larger  $v_2$ , it reaches the final value also sooner, indicating that it is the size of the overlapping region in the  $x$  direction which determines how fast the elliptical flow is generated in the collision.

To summarize, we have studied in this letter the elliptical flow generated during the partonic evolution in heavy ion collisions at RHIC energies. For medium range impact parameters, an appreciable elliptical flow has been found as a result of the initial spatial asymmetry and subsequent partonic rescattering. The magnitude of the elliptical flow shows a strong dependence on the parton-parton scattering cross section, demonstrating the importance of dissipative corrections to idealized hydrodynamic expectations. The finite parton elliptical flow is expected to lead to an initial hadron matter with an asymmetric azimuthal momentum distribution. This is different from heavy ion collisions at lower energy, such as the SPS, where the hadronic evolution starts with an approximately isotropic azimuthal momentum distribution in the nuclear overlapping region. Since the spatial asymmetry is relatively smaller during the hadronic evolution in heavy ion collisions at RHIC, one does not expect that hadronic rescattering will generate appreciable elliptical flow [7] and thus should not significantly modify the initial partonic elliptical flow.

In this first study we have not yet investigated the effects due to different initial conditions for the partonic matter. For example, the turbulent glue initial conditions given by the

HIJING model [14] may lead to a different value for the elliptical flow as obtained here using a thermal one. A quantitative study of effects due to both the hadronic rescattering and the initial parton distribution is underway by using a transport model that takes results from the HIJING model [11] as input to the ZPC parton cascade model [9] and then includes the hadron cascade via the ART model [6]. Such a comprehensive study will allow us to find quantitatively the sensitivity of elliptical flow on the parton-parton scattering cross section, thus making it possible to extract valuable information on the properties of the hot dense parton matter formed in the initial stage of ultrarelativistic heavy ion collisions.

We thank B.A. Li for helpful discussions. The work of BZ and CMK was supported in part by the National Science Foundation under Grant No. PHY-9870038, the Welch Foundation under Grant No. A-1358, and the Texas Advanced Research Program. The work of MG was supported by the U.S. Department of Energy under contract No. DE-FG02-93ER40764.

## REFERENCES

- [1] M. Gyulassy, Nucl. Phys. **A590** (1995) 431c, and references therein.
- [2] J.W. Harris and B. Müller, Ann. Rev. Nucl. Part. Sci. **46** (1996) 71, and references therein.
- [3] D. Rischke, Nucl. Phys. **A610** (1996) 88c; J.-Y. Ollitrault, Nucl. Phys. **A638** (1998) 195c, and references therein.
- [4] M. Gyulassy, K.A. Frankel, and H. Stöcker, Phys. Lett. **B110** (1982) 185; P. Danielewicz and M. Gyulassy, Phys. Lett. **B129** (1983) 283.
- [5] C.M. Ko and G.Q. Li, J. Phys. **G22** (1996) 1673; G.Q. Li, C.M. Ko, and B.A. Li, Phys. Rev. Lett. **74** (1995) 235; G.Q. Li and C.M. Ko, Nucl. Phys. **A594** (1995) 460.
- [6] B.A. Li and C.M. Ko, Phys. Rev. C **52** (1995) 2037, Phys. Rev. C **58** (1998) R1382, Nucl. Phys. **A601** (1996) 457.
- [7] H. Sorge, Phys. Rev. Lett. **78** (1997) 2309; nucl-th/9812057.
- [8] J.-Y. Ollitrault, Phys. Rev. D **46** (1992) 229.
- [9] B. Zhang and Y. Pang, Phys. Rev. C **56** (1997) 2185; B. Zhang, M. Gyulassy, and Y. Pang, Phys. Rev. C **58** (1998) 1175; B. Zhang, Comput. Phys. Commun. **109** (1998) 193; **111** (1998) 276 (E).
- [10] M. Gyulassy, Y. Pang, and B. Zhang, Nucl. Phys. **A626** (1997) 999;
- [11] X.N. Wang, M. Gyulassy, Phys. Rev. D **44** (1991) 3501; M. Gyulassy, X.N. Wang, Comput. Phys. Commun. **83** (1994) 307.
- [12] J.-Y. Ollitrault, Nucl. Phys. **A590** (1995) 561c; W. Reisdorf and H.G. Ritter, Annu. Rev. Nucl. Part. Sci. **47** (1997) 663.
- [13] C. Hartnack, H. Stöcker, and W. Greiner, Phys. Lett. **B215** (1988) 33; Y. Pang, Pro-

ceedings of RHIC'96: Theory Workshop on Relativistic Heavy Ion Collisions, edited by S. Kahana and Y. Pang, (1996) 193.

[14] M. Gyulassy, D.H. Rischke, and B. Zhang, Nucl. Phys. **A613** (1997) 397.



## List of Figures

1	Time evolution of $v_2$ coefficient for different effective parton scattering cross sections in Au-Au collisions at $\sqrt{s} = 200$ AGeV with impact parameter 7.5 fm. Filled circles are cascade data, and dotted lines are hyperbolic tangent fits to the data. . . . .	10
2	Time evolution of $v_2$ and $v'_2$ coefficients from the same reaction as in Fig. 1 for $\sigma = 10$ mb and $b = 7.5$ fm. Filled circles are cascade data with statistical errors, and dotted lines are hyperbolic tangent fits to the data. . . . .	11
3	Impact parameter dependence of $v_2$ and $v'_2$ . Filled circles are for $v'_2$ and open circles are for $v_2$ . The lines are splines to guide the eyes. . . . .	12
4	Time evolution of $v_2$ for different impact parameters. The cross section is taken to be 3 mb. Filled circles are cascade data, and dotted lines are hyperbolic tangent fits to the data. . . . .	13

# FIGURES

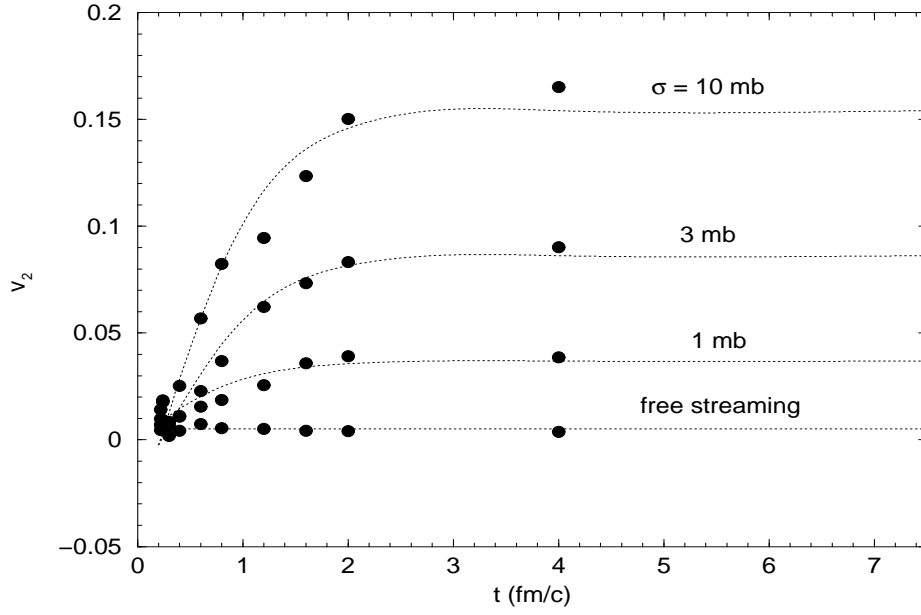


FIG. 1. Time evolution of  $v_2$  coefficient for different effective parton scattering cross sections in Au-Au collisions at  $\sqrt{s} = 200$  AGeV with impact parameter 7.5 fm. Filled circles are cascade data, and dotted lines are hyperbolic tangent fits to the data.

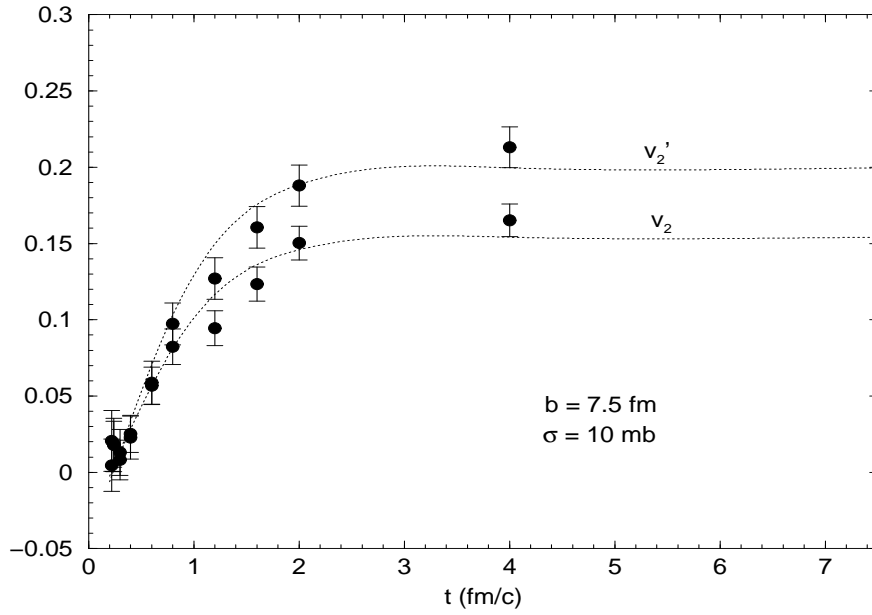


FIG. 2. Time evolution of  $v_2$  and  $v_2'$  coefficients from the same reaction as in Fig. 1 for  $\sigma = 10$  mb and  $b = 7.5$  fm. Filled circles are cascade data with statistical errors, and dotted lines are hyperbolic tangent fits to the data.

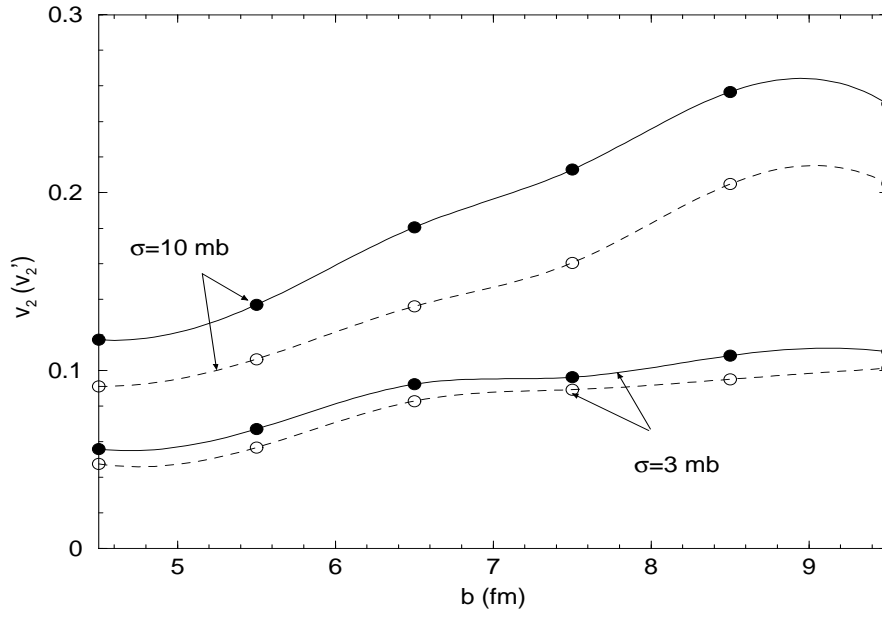


FIG. 3. Impact parameter dependence of  $v_2$  and  $v_2'$ . Filled circles are for  $v_2'$  and open circles are for  $v_2$ . The lines are splines to guide the eyes.

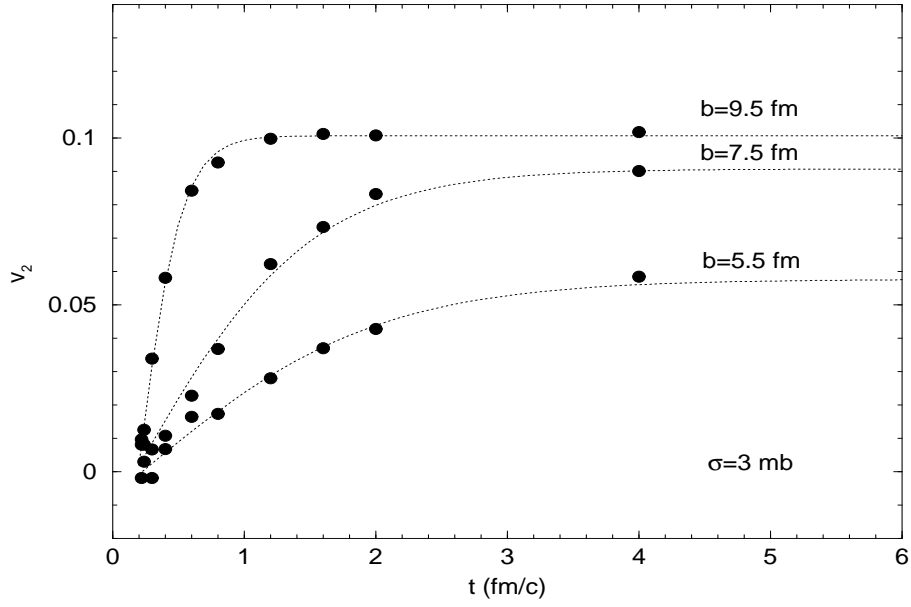


FIG. 4. Time evolution of  $v_2$  for different impact parameters. The cross section is taken to be 3 mb. Filled circles are cascade data, and dotted lines are hyperbolic tangent fits to the data.